

Guidelines for effective microwave breast imaging: a numerical assessment against 3D anthropomorphic phantoms

I. Catapano*, L. Crocco*, L. Di Donato*, G. Angiulli[†], S. Tringali[†], T. Isernia[†], O. M. Bucci*[‡]

* National Research Council - Institute for Sensing of the Environment
via Diocleziano 328, 80124 - Napoli, Italy,
(catapano.i,crocco.l,didonato.l)@irea.cnr.it

[†] University Mediterranea of Reggio Calabria - Dep. of Informatics, Mathematics, Electronic and Transportation,
loc T. (giovanni.angiulli,salvo.tringali,tommaso.isernia)@unirc.it

[‡] University of Naples Federico II - Dep. of Biomedical, Electronic and Telecommunication Engineering,
Via Claudio 21, 80125 - Napoli, Italy
bucci@unina.it

Abstract—Microwave tomography has gained an increasing attention as a tool for breast cancer screening, owing to its ability of providing a quantitative estimation of the electromagnetic features of the human tissues. In this respect, the design of the experimental setup is a critical issue, since it may affect the complexity of the involved inverse scattering problem and therefore the reliability of the screening. Aim of this communication is to propose some guidelines to properly set the matching fluid. These are derived with reference to an one dimensional simplified breast model, which does not take into account the high heterogeneity of a real female breast. Hence, a preliminary numerical assessment of their effectiveness against three-dimensional anthropomorphic phantoms is given.

I. INTRODUCTION

Breast cancer is one of the most frequent causes of death among women and its early detection is crucial to improve the effectiveness of medical treatments, while reducing their costs [1]. Hence, the development of diagnostic tools, suitable for large scale screening and able to provide accurate images, has gained an increasing attention. In this framework, growing interest is currently addressed towards microwave imaging (MI) techniques, which are in principle capable of providing a morphological and functional characterization of the investigated tissues [2]. However, this is not a trivial goal since it involves the solution of a non-linear and ill-posed inverse scattering problem [3].

Recently, several efforts have been done in developing imaging strategies for detecting suspicious anomalies and retrieving their dielectric features [4], [5], [6]. Unfortunately, the proposed imaging strategies mainly adopt a simplified model of the breast and/or require enforcement of *a priori* information (f.i., the skin thickness), usually not available in practice, due to the high variability of human tissues and female breast's structure. As a consequence, a statement of the actual performances offered by MI in the framework of breast cancer screening is still an open issue.

In this respect, it is worth to note that, unlike what happens in other cases (such as, f.i., subsurface imaging), the experimental scenario for breast imaging is, to some extent, a *degree of freedom*. Therefore, its design may be exploited to act on the difficulty of the inverse problem, thus improving the overall capabilities of a MI diagnostics tool. In particular, a key issue is the choice of the fluid, in which the breast can be immersed, as it may help the coupling between the incident field and the internal structures of the breast. In the literature, such an aim has been pursued by adopting oil or mixtures of glycerine and water [4], [5], [6]. On the other hand, these choices seem to be based on empirical considerations and does not take into account the role of the matching fluid onto the achievable resolution as well as on the "difficulty" of the inverse problem at hand.

By relying on our previous knowledge on factors affecting accuracy and effectiveness of MI techniques [7], [8], [9] a study aimed at defining some guidelines to select the matching fluid, the working frequency range and the number of transmitting and receiving probes in a simulated breast imaging experiment has been recently proposed in [10]. As shown through numerical results, the fulfilment of these guidelines indeed allows to assure the reliability of the reconstructions [10]. On the other hand, the guidelines to select the matching fluid have been derived and verified a posteriori with respect to a simplified 2-D, although realistic, breast phantoms derived from realistic magnetic resonance images (MRI) were considered. Hence, the question arises of addressing this choice in the more realistic three-dimensional case.

This communication deals with this problem. In particular, to discuss how the choice of matching fluid affects the scattering experiment, we report the synopsis of an extensive full-wave simulation campaign carried out on realistic healthy breast phantoms obtained from MRI given in [11].

The paper is organized as follows. A simple model to address the choice of the matching fluid is summarized in Section II.

The three dimensional realistic breast phantoms are described in Section III together with the mathematical formulation of the forward scattering problem. Finally, the effectiveness of the guidelines arising from the simple model of Section II is assessed in Section IV by means of several numerical simulations. Conclusions and future work follow.

II. A SIMPLE MODEL FOR CHOOSING THE MATCHING FLUID

Some guidelines to select the matching fluid have been already given in [10] as far as the two dimensional scalar case is concerned. In this framework, to maximize the incident power, a matching fluid whose conductivity is as low as possible has been suggested, while its relative permittivity, ϵ_f , has been selected by computing the reflection coefficient, Γ_r , at the fluid-skin interface. This task has been faced by observing that the breast can be considered angularly homogeneous and the skin layer is very thin compared to the other involved electrical lengths. Moreover, the internal breast structure itself is large in terms of the probing wavelength and may be approximatively considered as an homogeneous media, whose electric features depend on the amount of its adipose tissue. Accordingly, a female breast can be simply modeled as an one dimensional three-layer structure. Hence, by schematizing the incident field as a plane wave normally impinging on the fluid-skin interface, an easy way to evaluate Γ_r is to consider the equivalent transmission line. By doing so, for a fixed thickness of the skin layer, maps of the amplitude of Γ_r as a function of ϵ_f and the frequency have been obtained for three different types of breast, i.e., breast with 0 – 30%, 31 – 84% and 85 – 100% of adipose tissue.

Similar reasonings can be repeated to tackle the three dimensional vectorial case. In particular, one can still compute $|\Gamma_r|$ as a function of ϵ_f and f by means of the equivalent transmission line, provided it accounts for the angle of the impinging wave, θ_i , as well as the field polarization. Therefore, for each breast type, maps of $|\Gamma_r|$ parameterized with respect to θ_i and the field polarization are obtained. As an example, let us consider a breast with 85 – 100% of adipose tissue having damp skin layer 1.5mm thick. Figure 1.a shows the map of $|\Gamma_r|$ for a normal incidence and both the field polarizations, while figs.1.b,c give those concerning an incident angle $\theta_i = 30^\circ$ and the transverse electric and magnetic polarizations, respectively. It worth to note that these maps do not significant change when the thickness of the skin is in the range [1.5 – 2.5]mm. Moreover, as in the two dimensional case [10], the considered breast type mainly constrains the choice of ϵ_f in all the considered frequency range. Hence, we focus our attention on it to chose a suitable matching fluid.

Figures 1.a-c show that there are several possible choices for both ϵ_f and f . However, by accounting for the maps of $|\Gamma_r|$ for $\theta_i \in [0^\circ - 30^\circ]$; in the frequency range 1 – 4GHz, it proves convenient to select a fluid having $\epsilon_f \leq 30$, in order to assure that, for $\theta_i < 30^\circ$, a satisfactory fraction of the incident field actually impinges on the internal breast tissues, whatever the field polarization is. This statement is corroborated in Section

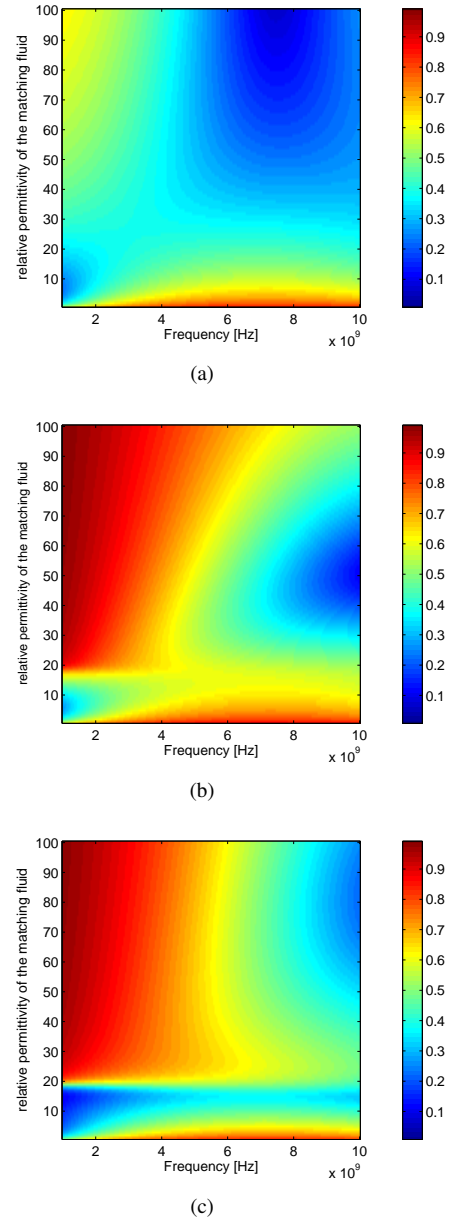


Fig. 1. Amplitude of the fluid-skin interface reflection coefficient for breast with 85 – 100% adipose tissue: a) normal incidence transverse electric and magnetic polarizations; b) $\theta_i = 30^\circ$ transverse electric polarization; c) $\theta_i = 30^\circ$ transverse magnetic polarization.

IV, where the effects of the matching fluid on the total electric field inside 3-D realistic breast phantoms are discussed. On the other hand, the effects of ϵ_f and f on the imaging process have also to be taken into account. As a matter of fact, they affect not only the scattering from internal tissues, but also the electrical size of the overall investigated scenario as well as those of possibly tumoral inclusions. In particular, it is worth to consider that the achievable spatial resolution of an MI approach mainly depends on the background wavelength

λ_b , being in the order of $\lambda_b/4$ ¹ [12]. On the other hand, the lower is λ_b the larger is the size of the scatterers as well as the maximum value of the electric contrast. As a consequence, since the *degree of non linearity* of the data to unknown relationship grows with the electrical size of the investigated domain as well as with the electric contrast the difficulty of the inverse scattering problem becomes higher [7], [9]. Therefore, one should choose ϵ_f as a trade-off between the need to assure a good resolution and the necessity to avoid local minima. In addition, to assure the robustness of the inversion approach against local minima it is also convenient to collect multifrequency data starting at 1GHz.

III. THE FORWARD SCATTERING PROBLEM

A. Numerical Breast phantoms

In order to take into account the complex structure of a female breast, the numerical breast phantom repository given in [11] has been exploited. Such a database provides anatomically realistic 3-D numerical phantoms from MRI, which well represent the heterogeneity of the healthy breast tissues. As a matter of fact, it deals with four classes of female breasts: mostly fatty, scattered fibroglandular, heterogeneously dense and very dense breasts. In the following, we focus our attention on two phantoms having opposite characteristic, i.e., a mostly fatty breast (*breastID* : 071904 in [11]) and a very dense one (*BreastID* : 012304 in [11]). Their dispersive behavior has been described accordingly the tissues classification given in [14] and the single pole Cole-Cole model. In particular, the frequency-dependent dielectric properties of each pixel of the considered breast phantoms have been assigned following the instructions provided in [11] and assuming and dropping $\exp(j\omega t)$ as time dependence.

Figures 2.a-b and figs. 3.a-b show the relative permittivity and conductivity profiles obtained at 1GHz for the above phantoms, respectively.

B. Mathematical formulation

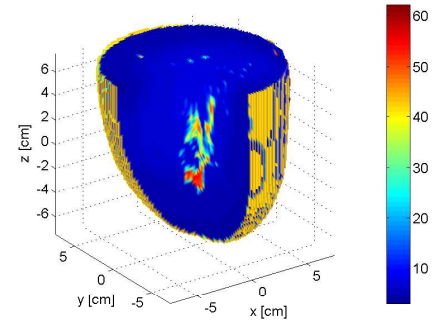
Let us assume the breast to be immersed into a beaker filled with a matching fluid. The primary source of the scattering experiment are z -directed elementary dipoles located inside the beaker on a circumference Γ centered at the origin of the coordinate reference system. The scattered field is measured in N_m measurement point located on Γ .

Let Ω denote a cubic domain containing the breast, at a fixed angular frequency, ω , and for each primary source, the total field in the generic point $\mathbf{r} \in \Omega$ is given as:

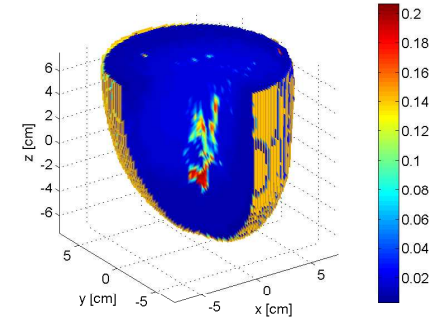
$$\mathbf{E}(\mathbf{r}) = \mathbf{E}_{inc}(\mathbf{r}) + k_b^2 \int_{\Omega} \mathbf{G}(\mathbf{r}, \mathbf{r}') \chi(\mathbf{r}') \mathbf{E}(\mathbf{r}') d\mathbf{r}', \quad (1)$$

where k_b is the wave number in the matching fluid and χ is the scalar electric contrast function which relates the complex

¹This value is the exact one that arises for the Born Approximation [12], whereas it can be considered as an upper bound for the general (non-linear) case, if one takes into account that the number of degrees of freedom of data enforces a limit on the maximum number of parameters (describing the inclusions) which can be safely extracted [13].

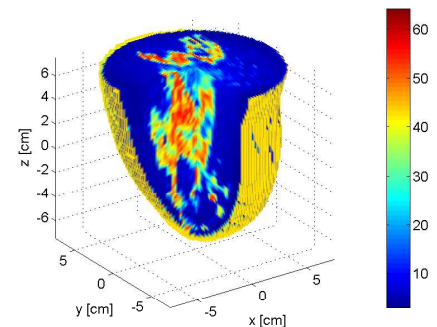


(a)

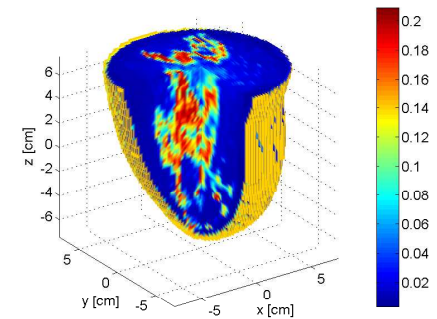


(b)

Fig. 2. Mostly fatty breast: a) relative permittivity profile; b) conductivity profile



(a)



(b)

Fig. 3. Very dense: a) relative permittivity profile; b) conductivity profile

permittivity of the breast $\epsilon(\mathbf{r})$ and that of the matching fluid, ϵ_f :

$$\chi(\mathbf{r}) = \frac{\epsilon(\mathbf{r})}{\epsilon_f(\mathbf{r})} - 1. \quad (2)$$

In eq.(1), \mathbf{E}_{inc} denotes the incident field in Ω , i.e., the field without the breast, and \mathbf{G} is the diadic Green's function for a homogeneous medium, whose electric parameters are those of the matching fluid [15].

The scattered field in $r_m \in \Gamma$ is given as:

$$\mathbf{E}_s(\mathbf{r}_m) = k_b^2 \int_{\Sigma} \mathbf{G}(\mathbf{r}_m, \mathbf{r}) \chi(\mathbf{r}') \mathbf{E}(\mathbf{r}') d\mathbf{r}. \quad (3)$$

The fields \mathbf{E} and \mathbf{E}_s have been computed by means of a method of moments based full wave 3D forward solver.

IV. NUMERICAL ANALYSIS

Aim of this section is to discuss the effectiveness of the guidelines given in Section II by investigating how the choice of the matching fluid affects the behavior of the total field inside the female breast, i.e, in the tissues behind the skin layer. In the following the support of the internal breast tissues is named Θ and 4 z -directed dipoles $\pi/2$ angularly spaced on Γ are assumed as primary sources of the scattering experiments. Γ is located in the plane $z = 0$ cm and has radius equal to 20 cm, moreover the working frequency is set at 1 GHz.

Let us consider the primary source located in $(0, 20, 0)$ cm and both the breast phantoms described in Section III.

As an objective index to compare different matching fluids, for each primary source, let us consider the power of the total field in Θ normalized to the power of such a field in Ω .

$$\delta = \frac{\sum_i^{N_{voxel,\Theta}} [|E_x|^2 + |E_y|^2 + |E_z|^2]}{\sum_i^{N_{voxel,\Omega}} [|E_x|^2 + |E_y|^2 + |E_z|^2]} \quad (4)$$

where $N_{voxel,\Theta}$ and $N_{voxel,\Omega}$ are the number of voxels in Θ (i.e. in the breast without the skin) and in Ω , respectively.

For the mostly fatty breast phantom and the very dense one described in the previous Section, the values of δ concerning three different fluids having null conductivity and relative permittivity equal to $\epsilon_f = 2.5$, $\epsilon_f = 15$ and $\epsilon_f = 30$ are given in table I and table II, respectively. These tables corroborate that, according to the maps of the reflection coefficient, the values of δ concerning a fluid having $\epsilon_f = 30$ is always lower than those concerning the other fluids. However, since $\epsilon_f = 30$ provides a sufficiently low $|\Gamma_r|$ for $\theta_i < 20^\circ$ whatever the field polarization is, all the considered fluids assure that the internal region of the breast takes actually part in the scattering phenomenon. This statement is stressed by figs.4.a,b, figs.5.a,b and figs.6.a,b, which show the plot of the normalized magnitude of the total field in Θ for the above considered fluids. By observing these figures it is, indeed, apparent that a satisfactory portion of the total field is concentrated in Θ and actually affects the field scattered on Γ .

On the other hand, since a matching fluid having $\epsilon_f = 15$ provides values of δ comparable with those concerning $\epsilon_f = 2.5$ but a higher resolution, we can conclude that a matching fluid having ϵ_f around such a value is preferable.

TABLE I
 δ - MOSTLY FATTY BREAST

	source 1	source 2	source 3	source 4
$\epsilon_f = 2.5$	0.4924	0.4357	0.4752	0.4397
$\epsilon_f = 15$	0.4256	0.4545	0.4031	0.4637
$\epsilon_f = 30$	0.3666	0.4172	0.3442	0.3894

TABLE II
 δ - VERY DENSE BREAST

	source 1	source 2	source 3	source 4
$\epsilon_f = 2.5$	0.5373	0.5271	0.5618	0.4768
$\epsilon_f = 15$	0.5150	0.4967	0.4819	0.4484
$\epsilon_f = 30$	0.3971	0.4721	0.4194	0.4163

V. CONCLUSIONS

Guidelines to set the matching fluid have been given by assuming a simplified 1-D breast model and dealing with the equivalent transmission line. Then, their effectiveness against realistic 3-D phantoms has been numerical assessed at 1GHz by reasoning on the behavior of the total field inside the phantoms.

Future work will be addressed to further investigate the reliability of the proposed criteria in a wide range of frequencies and in exploit them to properly cope with the breast imaging problem and the early detection of tumoral inclusions.

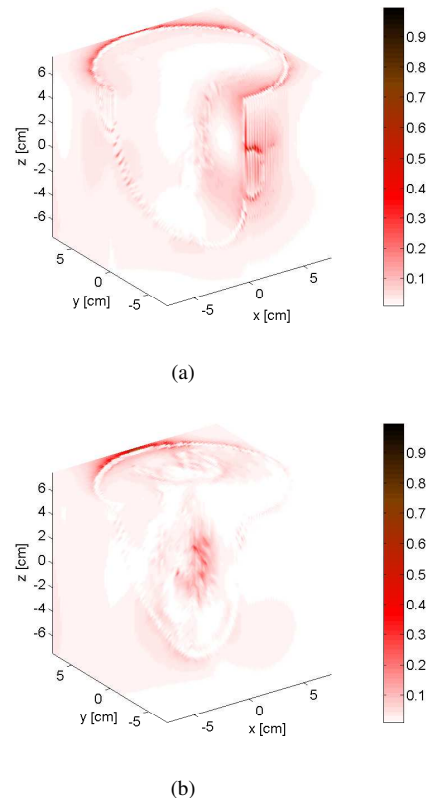
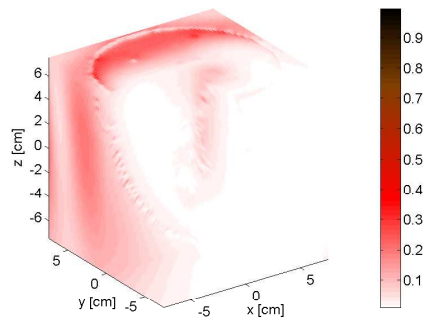
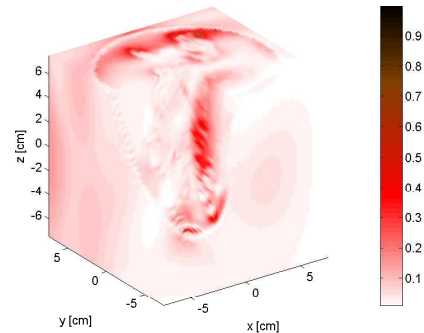


Fig. 4. Map of the magnitude of total field in Ω for $\epsilon_f = 2.5$: a) mostly fatty breast; b) very dense breast



(a)



(b)

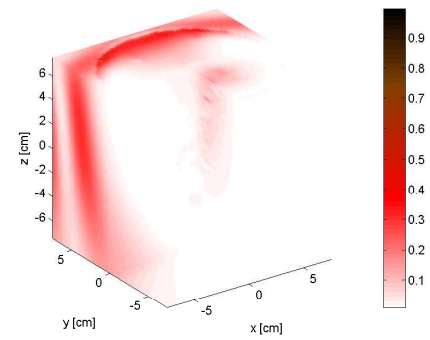
Fig. 5. Map of the magnitude of total field in Ω for $\epsilon_f = 15$: a) mostly fatty breast; b) very dense breast

ACKNOWLEDGMENT

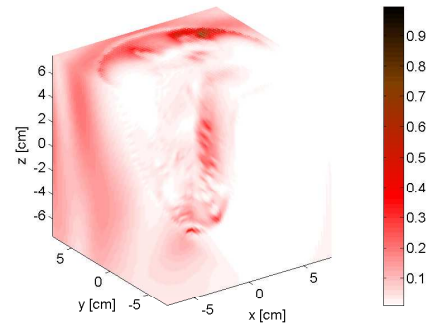
This work has been partially supported by the Italian Ministry of Research under the Program PRIN 2007, "MANFIND: Magnetic Nanoparticles and Fields for Nanotechnologies and Diagnostics".

REFERENCES

- [1] Cancer Facts and Figures 2009, American Cancer Society, Inc., 2009.
- [2] E. C. Fear, P. M. Meaney, and M. A. Stuchly, "Microwaves for breast cancer detection," *IEEE Potentials*, 2003.
- [3] M. Bertero and P. Boccacci, *Introduction to Inverse Problems in Imaging*, Inst. of Physics, Bristol Philadelphia, UK, 1998.
- [4] T. Rubk, P. M. Meaney, P. Meincke, K. D. Paulsen, Nonlinear Microwave Imaging for Breast-Cancer Screening Using GaussNewton's Method and the CGLS Inversion Algorithm, *IEEE Trans. Antennas Propag.*, vol.55, pp.2320-2231, 2007.
- [5] C. Gilmore, A. Abubakar, W. Hu, T. M. Habashy, P.M. van den Berg, Microwave biomedical data inversion using the finite-difference contrast source inversion method, *IEEE Trans. Antennas Propag.*, vol.57, pp.1528-1538, 2009.
- [6] D. W. Winters, B. D. Van Veen, S. C. Hugness, A sparsity regularization approach to the electromagnetic inverse scattering problem, *IEEE Trans. Antennas Propag.*, vol.58, pp.145-154, 2010.
- [7] I. Catapano, L. Crocco, M. D'Urso, and T. Isernia, "On the effect of support estimation and of a new model in 2-D inverse scattering problems," *IEEE Trans. Antennas and Propag.*, vol. 55, pp. 1895-1899, 2007.
- [8] O. M. Bucci, L. Crocco, T. Isernia, Improving the reconstruction capabilities in inverse scattering problems by exploitation of close-proximity setup, *J. Opt. Soc. Am. A*, vol.16, pp.1788-1798, 1999.



(a)



(b)

Fig. 6. Map of the magnitude of total field in Ω for $\epsilon_f = 30$: a) mostly fatty breast; b) very dense breast

- [9] T. Isernia, L. Crocco, M. D'Urso, New tools and series for forward and inverse scattering problems in lossy media, *IEEE Geosci. Remote Sens. Letters*, vol.1, pp.327-331, 2004.
- [10] I. Catapano, L. Di Donato, L. Crocco, O. M. Bucci, A. F. Morabito, T. Isernia, R. Massa, "On quantitative microwave tomography of female breast", *Progress In Electromagnetics Research*, PIER 97, pp. 75-93, 2009.
- [11] E. Zastrow, S. K. Davis, M. Lazebnik, F. Kelcz, B. D. Van Veen, and S. C. Hagness, "Database of 3D grid-based numerical breast phantom for use in computational electromagnetics simulations," [http : //uwcem.ece.wisc.edu/home.htm](http://uwcem.ece.wisc.edu/home.htm).
- [12] M. Slaney, A. C. Kak, L. E. Larsen, Limitations of imaging with first-order diffraction tomography, *IEEE Trans. On Microwa. Theory Tech.*, vol.32, pp.860-874, 1984.
- [13] O. M. Bucci and T. Isernia, Electromagnetic inverse scattering: retrievable information and measurement strategies, *Radio Sci.*, vol. 32, pp. 2123-2137, 1997.
- [14] M. Lazebnik, L. McCartney, D. Popovic, C. B. Watkins, M. J. Lindstrom, J. Harter, S. Sewall, A. Magliocco, J. H. Booske, M. Okoniewski, S. C. Hagness, A large-scale study of the ultrawideband microwave dielectric properties of normal breast tissue obtained from reduction surgeries, *Phys. Med. Biol.*, vol.52, pp.2637-2656, 2007.
- [15] C. A. Balanis, *Advanced Enginering Electromagnetics*, John Wileys & Sons 1989.